MODELLING OF HAZARDOUS OPERATING MODES OF RUBBER-CORD COUPLING IN FEM ENVIRONMENT

Dmitrijs Gorbacovs, Pavels Gavrilovs, Janis Eiduks
Riga Technical University, Latvia
dmitrijs.gorbacovs@rtu.lv, pavels.gavrilovs@rtu.lv, janis.eiduks_2@rtu.lv

Abstract. Relevance of the research topic. During operation rubber-cord couplings with a toroidal shell form may fail. For the period from 2019 to 2023 (5 years) such failures amounted to more than 58 cases. According to a visual inspection of a large number of failed rubber-cord couplings, it was found that the cause of failure was a rupture of the side surface. The aim of this scientific article is to determine the forces and moments acting on the rubber-cord coupling, as well as the displacements of the shafts connected by the rubber-cord coupling in axial, radial and angular deflections. To determine the properties of the material, single tensile and cyclic tests of fragments of rubber-cord couplings were carried out. Based on the test results, a mathematical model of the material was determined. In the environment of the FEM software, the test results were compared with models of elastomeric materials and the most suitable model of elastomeric material that most accurately corresponded to the test results was selected. The calculated forces and torque effects were simulated, and the effects of radial, axial and angular deflection and measured coupling deflections were simulated. The purpose of modelling is to identify dangerous operating modes and dangerous forms of the rubber-cord coupling loading during operation.

Keywords: rubber cord coupling, hazardous situations, FEM modelling.

Introduction

At the railway company JSC "Pasažieru vilciens" working on the Latvian railway, failures of toroid rubber cord couplings of electrical and diesel multiple unit trains periodically occur. To confirm the relevance of the problem, for a period of 5 years from 2019 to 2023 statistics of failures were collected, compiled and analysed [1] and it was found:

- for electric trains – failure of 54 rubber cord couplings;
- for diesel trains – failure of 4 rubber cord couplings.

The accumulated number of failures by years is shown in Figure 1.

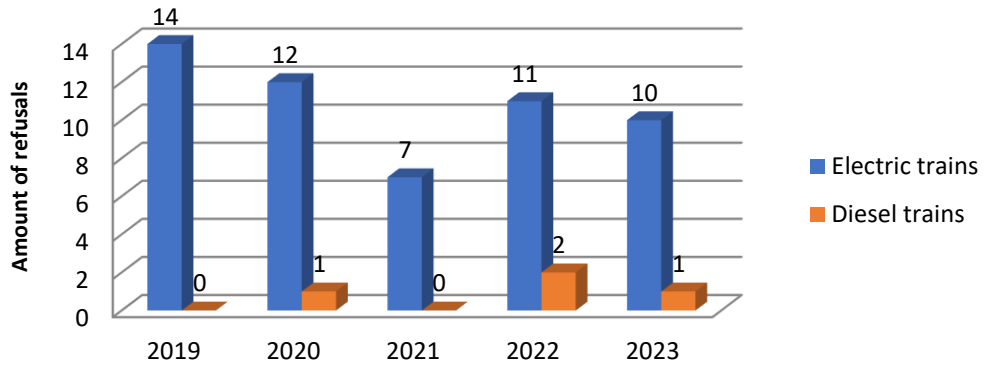

Fig. 1. **Failures of rubber cord couplings of electric and diesel trains**

Upon visual inspection of all failed 58 rubber cord couplings, it was found that the reason for the failure of 57 of them was the rupture of the side surface, and the failure of one coupling was the destruction of the upper surface. The general view of coupling failures is shown in Figure 2.

According to data received from JSC "Paszieru vilciens", the average cost associated with replacing one rubber-cord coupling is on average 589 EUR [2]. Due to the large number of failures and the high costs associated with replacing the coupling, the question arises, what is the reason for the disintegration of the side faces of the rubber cord couplings? The problem of rubber cord coupling failures is relevant worldwide.

The author [3] presented the results of theoretical and experimental studies of rubber-cord rotation shells of connected couplings. Based on the heat balance equation and the law of distribution of tangential stresses along the forming cylindrical shell, differential equations of temperature distribution

in the rubber-cord and metal parts of the coupling are obtained. The values of the damping coefficients and torsional rigidity of the rubber cord shell were obtained.

Fig. 2. **Types of failures of rubber-cord couplings:** a; b; c – rupture of the side surface; d – rupture of the upper surface

The authors [4] proposed a new method for calculating the oxygen consumption by rubber, which is applied to the oxygen consumption of various parts of the tire. To reduce IPLR of a tire, two approaches are used based on the design of the inner lining. This modelling method can predict the IPLR of tires not only in a steady rolling state, but also in a static state and even under aging conditions. It also provides an important modelling basis for tire aging studies and future tire life prediction.

The authors [5] in their paper present the results of experimental studies of stress-strain behaviour at the stages of hardening, as well as stabilization and reduction in the strength of rubber-cord shells under static loading. The influence of measurements of these characteristics on the dynamic load of the drive is shown. The physical processes of specific friction in a flexible coupling element have been considered. Diagrams were constructed for the dependence of specific friction on dynamic torque, vibration frequency, torsion angles and body temperature.

The author [6] in his paper presents experimental and calculated characteristics of the flexibility of an air spring and its dependence on the polytropic index and additional volume. The patterns of load distribution between air springs during their parallel operation to distribute the total load for the case when air springs are used as load-bearing elements are considered for various machines and units, as well as between transmission lines containing flexible couplings, where air springs and springs were installed as flexible elements.

In the work by the authors [7] is presented a description of the material properties of a rubber-cord elastic element necessary for assessing a pneumatic flexible element using the finite element method (FEM). The viscoelastic constitutive model of the rubber-cord composite is established by introducing the strain energy density function. To describe the properties of the rubber-cord element material, a curve is used, i.e. experimentally determined Mooney-Rivlin material curve. The corresponding constants were determined based on a tensile test of the rubber-cord element. The results are presented for the material of the pneumoelastic element of a differential pneumoelastic coupling with automatic adjustment.

Based on the results of a literature review, it was found that the problem of rubber-cord coupling failures is of scientific interest. While examining a large number of scientific works on the problems of rubber-cord coupling failures, some of which are presented in the literature review, it became clear that such issues as the influence of axial, angular and radial deflection, as well as the influence of the centrifugal force on the coupling in the FEM environment have not been yet considered. Since these issues have not been considered and research in this area has not been carried out, the authors of the work decided to conduct this type of research on the influence of deviations on reliable operation of the rubber-cord coupling.

Materials and methods

Rubber-cord couplings operate in conditions where it is very difficult to achieve alignment of the shafts connected by the coupling. As a result, the coupling is subject to axial, radial and angular deflections, and also operates at different ranges of torque and angular velocities. In this regard it is necessary to carry out modelling of various operating modes using the finite elemental modelling method in the FEM SolidWorks program.

1. Determination of axial radial and angular deviations of couplings during operation

In the period from 2021-2023, in order to check the compliance of the deviations of the rubber cord coupling shafts with the requirements [8], the coupling deviations of 30 motor cars in operation were measured when the mileage was 100÷200 ±5% thousand km. Measurements were made for 70 couplings at these mileage values. To ensure the best accuracy of the measurement, measurements were made in three places along the coupling arc: 0°; 90°; 180°. Measurements of axial, radial and angular deviations of coupling shafts were made using a special gauge with an accuracy class of ±0.1 mm. The measurement locations of the rubber cord coupling are shown in Figure 3.

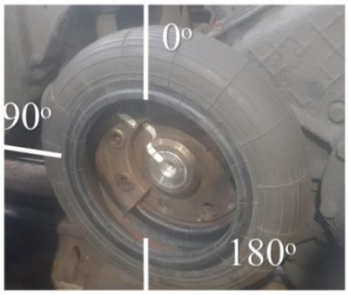

Fig. 3. **Rubber cord coupling measurement locations**

The measurement data of 70 rubber cord couplings are summarized in Table 1.

Table. 1

Coupling displacement measurement data 2021-2022

Coupling displacement	Radial displacement, mm	Axial displacement, mm	Angular displacement, degrees
Mean measured value	1-15	2-16	0 ± 4°
Maximum allowed value	15.0	20.0	4.0

The following graphs were obtained as a result of the deviation measurement data analysis for the parameters indicated in Table 1 (Figure 4).

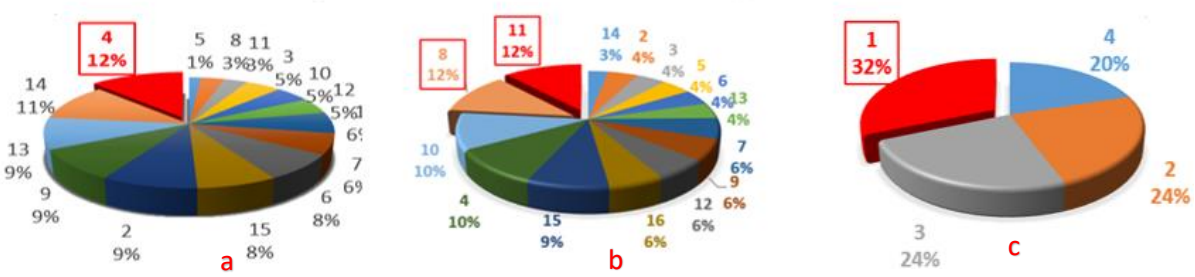

Fig. 4. **Radial (a), axial (b) and angular (c) deflection measurement data**

Analyzing the data of inclination angles, cases of significant deformations of flexible couplings in radial, axial and angular directions were found.

As a result of the measurement data analysis, it was found that the most common occurrences in operation are:

1. Deviation of 4 mm in the radial direction (Figure 4 a). The number of such cases is 8 cases or 12%.
2. Deviation of 11 mm and 8 mm in axial displacement (Figure 4 b). The number of such cases is 16 cases or 22.85%. On the graph in Fig. 4b they are shown in red and brown.
3. 1 mm deviations in angular displacement are 22 cases or 32%. On the graph in Figure 4 c it is shown in red.

Based on the results of measuring the axial, radial and angular deviations of the coupling, it was stated that on many couplings the deviations are significant, and 8% of couplings in radial deviation,

on the graph in Figure 4 a it is shown in red, and 20% of couplings in angular deviation, shown on the graph in Figure 4 c in blue, have a critical deviation parameter [8].

2. Determination of the material mechanical properties and performing simulations in the FEM environment

To determine the mechanical properties of the material, cyclic and single-tensile tests were performed on 6 fragments of rubber-cord couplings. The general view of fragments 1 and 2 is presented in Figure 5.

Fig. 5. **General view of fragments of rubber-cord couplings**

Data from the results of single-breaking and cyclic tests are presented in Tables 2 and 3.

Table 2

Coupling fragment No. 1; 4 tests at single breaking loads

Force, N	Deformation, *L* mm	Stress σ, MPa	Relative deformation, ε
0	0	0.0	0.0
193	4.0	0.1	0.1
2012	51.6	1.3	0.9
3017	68.5	1.9	1.1
5002	88.3	3.2	1.5
14580	150.0	9.3	2.5
15435	156.0	9.8	2.6
14400	160.0	9.1	2.6

Table 3

No. 2; 3 and No. 5; 6 coupling fragment tests under cyclic loads

Force, N	Deformation, *L* mm	Stress σ, MPa	Relative deformation, ε
0	0	0.00	0.00
579	4.67	0.37	0.08
1623	26.18	1.03	0.44
2802	48.00	1.78	0.80
4578	79.00	2.91	1.32
6375	101.00	4.05	1.68
7248	114.00	4.60	1.90
7667	126.00	4.87	2.10
7031	132.00	4.46	2.20
6118	138.00	3.88	2.30

In order to create a numerical model of the coupling material, a comparative analysis of the results of several tests was carried out for stress dependence on the relative deformation $\sigma = f(\varepsilon)$ [9]. In order to confirm the accuracy of the results, the test results were approximated with a polynomial function and the resulting (summarised) test graph for the dependence of stress on relative deformation was constructed [10-11].

Data in Table 2 and 3 was obtained from the results of a series of single-axle cyclic and tensile tests of rubber-cord coupling samples. The accuracy of the data obtained as a result of the experiments is

characterized by the measurement error, which, according to the passport data of the tensile testing machine is ± 0.5% of the measurement results. The results of calculations of stress σ and relative elongation ε were calculated with an accuracy of one hundredth (0.01).

The 6th order polynomial was chosen based on the results of the smallest value of the standard deviation R2 (Fig. 6).

The measurement error of a ZwickRoell tensile testing machine equipped with a force sensor X forse HP according to the passport data is ± 0.5% of the measurement results.

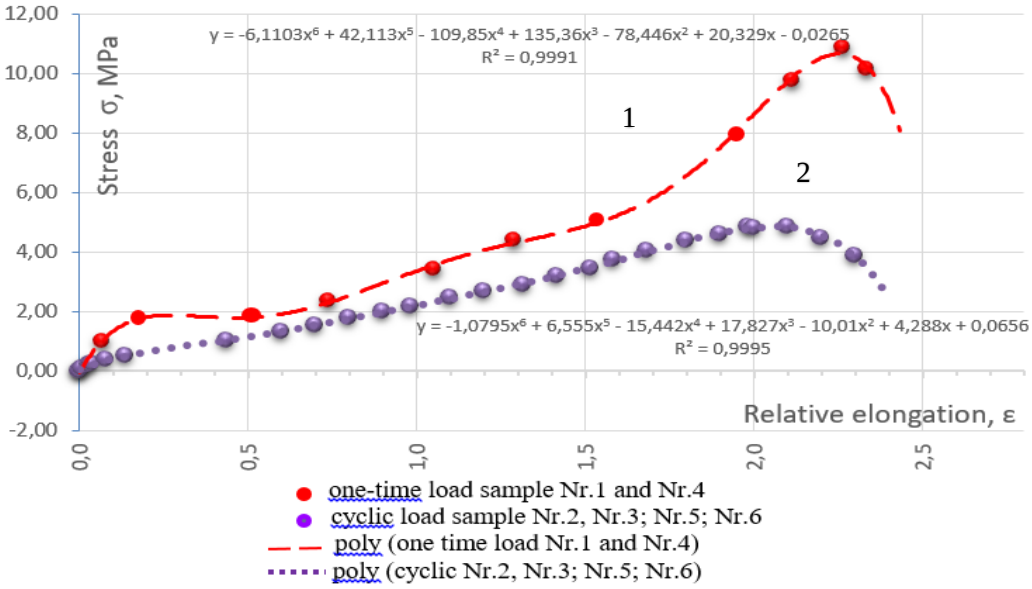

Fig. 6. **Comparison of unilateral tensile test results**

SolidWorks software for creating a calculation model

Based on the obtained results, the evaluation of the mechanical properties of the rubber samples of the surface layer was done and the results for the coupling shell fragments under single stretching and cyclic stretching loads were calculated. Calculation data is shown in Table 4.

Table 4

Average result of single stretching of coupling fragments No. 1 and No. 4, cyclic loading of fragments No. 2 and No. 5

Type of load	Limit of proportionality, MPa	Modulus of elasticity, MPa	Strength limit, MPa	Yield strength, MPa	Breakdown stress, MPa
	$\sigma_{0.2}$	E	σ_b	σ_y	Fracture
Single load	0.98	14.73	10.86	2.38	10.13
Cyclic load	0.102	15.24	4.87	0.50	3.88

The test results were compared in the Solid Works software with simulation data of 3 models of elastomeric materials:

- Mooney-Rivlin;
- Blatz Co;
- Nonlinear method.

The simulation results are presented in Figure 7.

Comparing the material test results of three elastomeric material models in SolidWorks, it was found that the Mooney–Rivlin elastomeric material model reflects the test results most accurate. Further we used the Mooney-Rivlin method for modelling the full rubber cord coupling shell.

Modelling the influence of axial radial and angular deflection on the coupling is show in Figure 8.

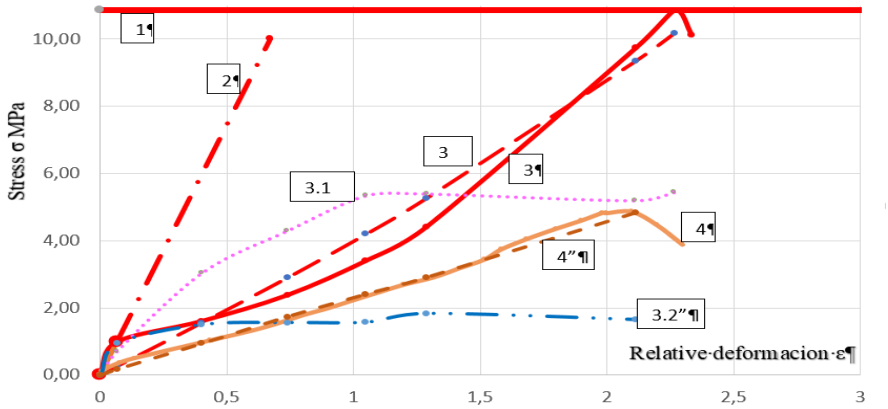

Fig. 7. **Results of modelling the stretching of fragments of the coupling shell by various methods:** 1 – ultimate strength (10.86 MPa); 2 – modulus of elasticity 14.73 MPa; 3 – experimental results – single stretching to rupture; 3" – results using the Mooney–Rivlin method for two constants; 3.1" – results using the Blatz method; 3.2" – results using the nonlinear elastic method; 4 – results of the experiment – cyclic tension to failure; 4" – results using the Mooney–Rivlin method in two constants by modifying the mesh of the model and the dimensions of the finite elements

Axial deviation

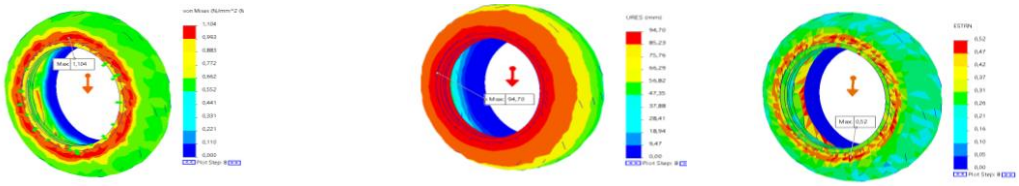

equivalent stresses equivalent displacement equivalent deformation

Angular deviation

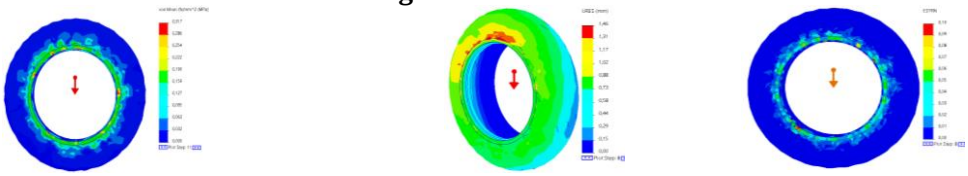

equivalent stresses equivalent displacement equivalent deformation

Radial deviation

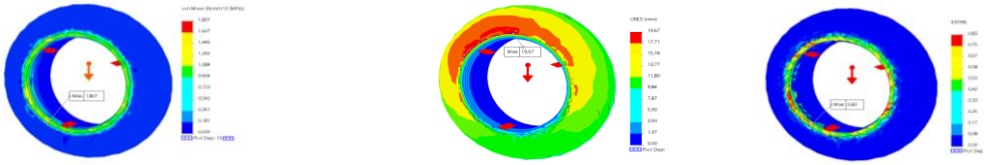

equivalent stresses equivalent displacement equivalent deformation

Fig. 8. **Modelling of maximum deviations and torque at 130 rpm**

Effect of centrifugal force on the coupling at different rpm

The effect of centrifugal forces at 690 rpm (which corresponds to the train speed 60km·h^{-1}) is shown in Figure 9.

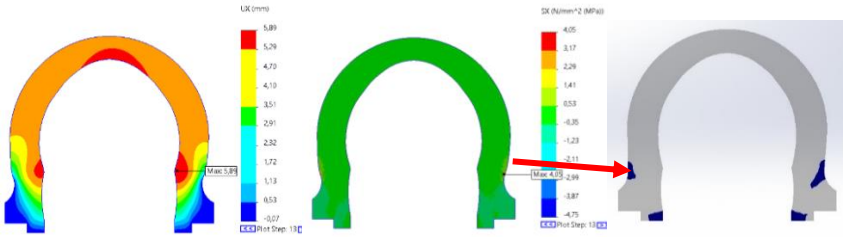

Fig. 9. **Effect of 690 rpm on the coupling**

The maximum stress at the place of fastening of the coupling at the flange is 4.05 MPa and spreads insignificantly in the cross section of the coupling.

The effect of centrifugal forces at 1670 rpm (which corresponds to the train speed 100km·h^{-1}) is shown in Figure 10.

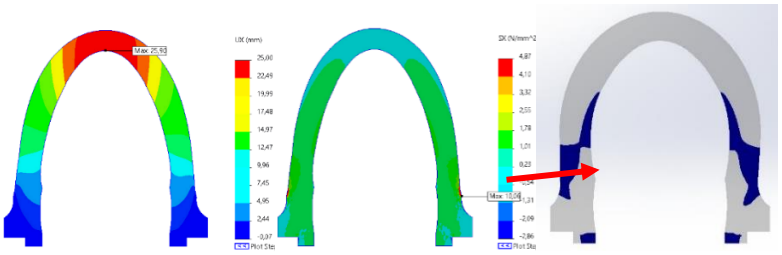

Fig. 10. **Effect of 1670 rpm on the coupling**

The maximum stress at the place of attachment of the coupling at the flange is 10.06 MPa and passes through the entire cross-section of the coupling.

Th effect of centrifugal forces at 1825 rpm (which corresponds to the train speed 120km·h^{-1}) is shown in Figure 11.

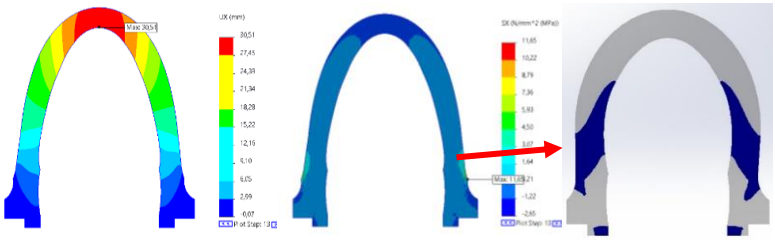

Fig. 11. **Effect of 1825 rpm on the coupling**

At 1825 rpm (120 km·h^{-1}) a critical radial movement of more than 30 mm was detected, which is very dangerous in the operating conditions of electric trains and can cause the upper part to collapse.

The maximum stress at the place of attachment of the coupling at the flange is 11.65 MPa spread through the entire cross-section and constitutes a large part of the cross-section of the side surface.

Conclusions

After creating the calculation model in the SolidWorks software tool, the following results were obtained using the selected Mooney-Rivlin elastomeric material models:

1. When modelling the maximum axial, radial and angular deviation data, it was found that the action of total stresses from axial, radial and angular deflections under cyclic loading is dangerous to the couplings and can cause damage of the side surface, because it is 3.21 MPa, which is more than 60% of the strength limit σ_b (4.87 MPa), which under cyclic loading causes the lateral surface to collapse.
2. Modelling different ranges of angular velocities in SolidWorks, it was found that at 1670 rpm, which is more than 110 km·h^{-1} of the train speed, the stress at the place of attachment of the coupling at the flanges exceeds the strength limit σ_b under cyclic load by more than 2 times and begins to spread over the entire cross-section of the coupling.
3. According to the modelling results, it is found that at axial, radial and angular deflection loaded areas coincide with the failure areas of in-service couplings.
4. It is proposed as an immediate action to limit the operation of rubber cord couplings above the train speed of 110 km·h^{-1} (1670 rpm). As a long-term solution for new couplings, the recommendation is to modify the geometric parameters of the rubber cord shell. Also, it is necessary to prevent continuous operation of the coupling at low rotation speed in the range up to 130 rpm.

Author contributions

D. G. was responsible for manuscript writing and editing, data analysis, content planning. P. G. was responsible for literature search, data collection and analysis, content planning. J. E. was responsible for manuscript editing, content planning and research guidance.

All authors have read and agreed to the published version of the manuscript.

References

[1] Summary of non-scheduled repairs of electric trains AS "Pasažieru vilciens" 2023 (template FT-22).

[2] Gorbacovs D., Gavrilovs P., Eiduks J., Strautmanis G. Failure Analysis of Rubber-Cord Couplings of ER2 Series Electric Trains 22th International Scientific Conference Engineering for Rural Development, 2023, pp. 313-320. ISSN 1691-5976.

[3] Evdokimov A. P., Investigation of Temperature Fields of Rubber-Cord Shells of Rotation of Connected Couplings of the Drives of Transport Vehicles, Journal of Machinery Manufacture and Reliability, 835, December 2023 – 842 p. DOI: 10.1134/S1052618823080058.

[4] Liang C., Sun Dong H., Li Chang D., Ji L., Ma T., Gao Z. Simulation Analysis of Tire Inflation Pressure Loss under Synergy of Temperature and Oxidation, International Journal of Automotive Technology, June 2023, pp. 693-703. DOI: 10.1007/s12239-023-0058-x.

[5] Evdokimov A. P., Shikhnabieva, T. Sh., Stress–strain behavior and specific friction of toric rubber-cord casings of flexible couplings, Journal of Machinery Manufacture and Reliability, 1 March 2017, pp. 199-203. DOI 10.3103/S1052618817020054.

[6] Vinogradov B. Mechanical systems with air spring flexible elements, Scientific Journal of Silesian University of Technology. Series Transport, pp. 199-207.

[7] Medvecká-Beňová S., Miková L., Kaššay P., Material prope rties of rubber-cord flexible element of pneumatic flexible coupling, Metalurgija, 1 January 2015, pp. 194-196 p., ISSN 05435846.

[8] ISO 14691:2008 Petroleum, petrochemical and natural gas flexible couplings for mechanical power transmission General-purpose applications 32 p.

[9] Ischuka O., Lomotko D., Freimane J., Sansyzbajeva Z. Main directions of improvement of the method for calculation of idle time of cars at technical stations Procedia Computer Science, 475 – 482 p., ICTE in Transportation and Logistics, ICTE 2018 Klaipeda1 January 2019.

[10] Ischuka O., Lomotko D., Gavrilovs P., Freimane J. Improvement of technology of operation for Daugavpils marshalling station by building the new receiving yard Transport Means - Proceedings of the International Conference, pp. 841-846.

[11] Ischuka O., Lomotko D., Eiduks J., Modelling of technology of disassembling and assembling of freight trains at marshalling yard, Transport Means - Proceedings of the International Conference, 24th International Scientific Conference on Transport Means 2020, Kaunas 30 September 2020 – 2 October 2020, pp. 463-468.